DECELERATION OF THE SOLAR WIND IN THE EARTH'S FORESHOCK REGION: ISEE 2 AND IMP 8 OBSERVATIONS

C.Bonifazi, G.Moreno

Laboratorio Plasma Spazio, CNR, Frascati, Italy

A.J.Lazarus, J.D.Sullivan

Center for Space Research, M.I.T., Cambridge (Mass.)

Submitted to J. Geophys. Res., January 1980

LPS-80-1

January 1980

ABSTRACT

The deceleration of the solar wind, in the region of the interplanetary space filled by ions backstreaming from the earth's bow shock, is studied using a two spacecraft technique. This deceleration, which is correlated with the "diffuse" but not with the "reflected" ion population, depends on the solar wind bulk velocity: at low velocities (below 300 km/s) the velocity decrease is $\sim$ 5 km/s, while at higher velocities (above 400 km/s) the decrease may be as large as 30 km/s. Along with this deceleration, the solar wind undergoes a deflection by $\sim$ 1° away from the direction of the earth's bow shock. The energy balance shows that the kinetic energy loss far exceeds the thermal energy which is possibly gained by the solar wind: therefore, at least part of this energy must go into waves and/or into the backstreaming ions.

1. INTRODUCTION

Perturbations of the solar wind protons in the "foreshock region", i.e. the region of the interplanetary space filled by ions backstreaming from the earth's bow shock, have been studied by several authors in the past few years. Since direct measurements of the backstreaming ions were restricted to relatively short periods of time, the presence of these particles was usually inferred from the long-period ($\sim$50 s) hydromagnetic waves associated with them. Studies of perturbations in the solar wind based on this indirect technique gave conflicting results:

(i) Feldman et al., 1974, using IMP 6 data, found that the thermal anisotropy of the solar wind protons was slightly lower in the region where the magnetic field lines were connected to the shock; on the other hand, the proton temperature did not exhibit any difference between the "connected" and the "unconnected" regions. (Note that backstreaming ions do not fill the whole "connected" region, see e.g., Greenstadt, 1972; Diodato et al., 1976).

(ii) Formisano and Amata, 1976, comparing Explorer 33 and HEOS 1 observations, found a decrease by $\sim$ 30 km/s of the solar wind bulk velocity in the foreshock region.

(iii) Auer et al., 1976, using HEOS 2 data, did not find evidence for any decrease of the solar wind velocity in the foreshock region; on the other hand, they reported a $\sim$ 13% decrease in the proton density and a $\sim$47% increase in the quantity $T_{//}\ B^2/N^2$.

(iv) Diodato and Moreno, 1977 performed a more extended, but still indirect, statistical analysis. Hourly averages of the solar wind proton parameters (density, bulk velocity, temperature) measured simultaneously by two spacecraft inside and outside the foreshock region were

used in that investigation. It was shown that studies of solar wind perturbations based on data from a single spacecraft (such as that performed by Auer et al.) could be heavily biased because of changes in solar wind conditions. None of the parameters considered exhibited significant variations in the foreshock region. It was pointed out, however, that minor modifications of the solar wind could have been obscured by the use of hourly averages.

It should also be recalled that a deceleration of the solar wind in front of the earth's bow shock has been discussed by Neugebauer, 1970: however, that phenomenon appears to be entirely different from the one dealed in the present paper, as it occurs just upstream of the shock's magnetic field gradient.

The ISEE 1 and 2 satellites have recently provided an opportunity to investigate in more detail the complex wave-particle interactions which dominate the plasma in the foreshock region. From these measurements it has become apparent that the ions which stream back from the earth's bow shock may be separated into two populations which are referred to as "reflected" and "diffuse" (Gosling et al., 1978). While the reflected population does not seem to interact significantly with the incoming solar wind, the diffuse ions are associated with low frequency hydromagnetic waves (Paschmann et al., 1979) as well as with time fluctuations of the parameters of solar wind protons (Bonifazi et al., 1979; Formisano et al., 1979). Bame et al., 1979, using data supplied by the LASL/MPI plasma experiment on board of ISEE 1, have also shown that the solar wind bulk properties are apparently altered in two respect by the presence of the diffuse (but not of the reflected) ion population:

(i) the average velocity decreases by 7-10 km/s;

(ii) the flow direction is deflected by $\sim$ 2 degrees away from the bow shock.

Data from a single spacecraft cannot, in general, distinguish between changes in the solar wind properties related to the presence of backstreaming ions and those which may be due to other causes: a bias, such as that discussed by Diodato and Moreno, 1977, could affect any analysis not involving simultaneous solar wind observations outside of and in the foreshock region. Thus, the results obtained by Bame et al., 1979, even though based on a large sample of data, could still be biased by changes in the incident solar wind.

The aim of the present report is to further investigate the problem of solar wind deceleration in the foreshock region. The two spacecraft technique will be applied using plasma measurements obtained simultaneously by the solar wind experiments on board of ISEE 2 and IMP 8. The plan of the paper is as follows:

In Section 2 we check the consistency of the proton parameters derived from the ISEE 2 and IMP 8 plasma experiments. In Sections 3 and 4 we investigate respectively the variations of the average solar wind velocity and flow direction in the foreshock region. The analysis confirms the results of Bame et al., 1979 and also suggests that the deceleration of the solar wind depends on its bulk velocity. Finally, in Section 5 we investigate whether the kinetic energy loss associated with the solar wind deceleration goes, at least partially, into a thermalization of the solar wind itself.

2. THE DATA SET

Our analysis is based on solar wind observations performed by ISEE 2 and IMP 8 during the period from November 3 to December 6, 1977. The plasma experiments on board of these satellites have been described by Bonifazi et al., 1978 (ISEE 2) and by Bellomo and Mavretic, 1978 (IMP 8).

The ISEE 2 EGD plasma experiment uses two hemispherical electrostatic analyzers to measure the positive ions as a function of azimuthal flow direction and of energy per unit charge, in the range from ∿ 50 eV/Z to ∿ 11 keV/Z. The experiment operates in two different modes which alternate automatically: all observations considered here were taken in the "wide energy spectrum" (WES) mode, which supplyies a full ion energy spectrum every ∿ 96 seconds. The basic moments of the distribution function of the solar wind protons (bulk velocity, azimuthal flow direction, density, most probable thermal speed) were derived through a procedure of numerical integration, outlined by Bavassano-Cattaneo et al., 1979.

The IMP 8 MIT plasma experiment uses a multigrid Faraday cup with slots to measure the angular and energy distributions of the positive ions in the range from ∿ 50 eV/Z to ∿ 7 keV/Z. A set of solar wind parameters is obtained every ∿ 60 seconds. The method of analysis consists in fitting a Maxwellian distribution to the data.

It is well known that substantial discrepancies often exist among solar wind parameters derived from different experiments (see, e.g., Moreno and Signorini, 1973). It is therefore necessary to check the consistency of the two sets of data to be compared.

Figures 1 and 2 show cross-comparisons of the values of proton bulk velocity (V), azimuthal flow direction (Φ), number density (N), most probable thermal speed (W) measured simultaneously by the two

spacecraft. Only periods when both satellites were in the undisturbed interplanetary space (i.e. outside the foreshock region) have been considered. Inspection of the plots shows:

(i) The bulk velocity measured by the two satellites (part (a) of Figure 1) differs systematically by 8 to 10 km/s ($V_{IMP\ 8}$ being larger than $V_{ISEE\ 2}$). On the other hand, the consistency of the two sets of data is ensured by the fact that the straight line best fitting the points has a slope of $\sim 45°$ ($\tan \alpha = 0.984$) and by the small value of the standard deviation ($\sigma = 4.3$ km/s).

(ii) The flow angles (part (b) of Figure 1) are, on the average, in close agreement, the best fit line being almost coincident with the "ideal" straight line passing through the origin and having a slope of 45°. The scatter of points is, however, larger than in the previous plot ($\sigma = 0.83°$).

(iii) Densities (part (a) of Figure 2) are rather poorly correlated ($\sigma = 4.5\ cm^{-3}$). On the average, a systematic difference of 2 to 3 cm^{-3} seems to be present ($N_{IMP\ 8}$ being larger than $N_{ISEE\ 2}$).

(iv) Concerning the thermal speeds (part (b) of Figure 2), the slope of the best fit straight line ($\tan \alpha = 0.633$) differs substantially from the "ideal" pattern. Nevertheless, the standard deviation of the points ($\sigma = 5$ km/s) indicates that the discrepancies between the two experiments do not exceed $\sim 20\%$ of the average value of W: therefore, any difference between the solar wind thermal speeds, at the locations of the two satellites, of that order of magnitude (or larger) should be observable.

3. SOLAR WIND DECELERATION

Decreases of the solar wind velocity, in presence of "diffuse" ions backstreaming from the Earth's bow shock, are often observed by ISEE 2, and confirm the finding of Bame et al., 1979. Panels (a) and (b) of Figure 3 show an example of solar wind deceleration obtained by the LASL/MPI plasma experiment on ISEE 1 and by the EGD experiment on ISEE 2. The results of both experiments agree in indicating that, when diffuse ions are detected (black bars in the figure), the bulk velocity not only fluctuates strongly, but also decreases, on the average, by ~20 km/s.

However, as pointed out in Section 1, observations of solar wind perturbations, based on data from a single spacecraft, may be misleading. In panel (c) of Figure 3 a case is shown which apparently contraddicts the proposed deceleration: in fact, for this event the solar wind bulk velocity undergoes an increase (rather than a decrease) when the diffuse ions are present. Even though relatively infrequent, the occurrence of events of this type points to the necessity of performing an analysis based on the two-spacecraft technique.

Figure 4 shows simultaneous measurements of the solar wind velocity performed by ISEE 2 and IMP 8. The following criteria were used to judge whether each satellite was in presence of the diffuse ions. For ISEE 2, the question was settled unambiguously because the EGD experiment clearly detects the fluxes of backstreaming particles and allows a distinction between the reflected and diffuse populations. On the other hand, the lower sensitivity of the IMP 8 plasma experiment usually prevents a direct observation of the backstreaming ions. Therefore for this satellite the following criteria were adopted:

(i) Knowledge of the interplanetary magnetic field direction (supplied by the UCLA magnetometer on board of ISEE 1), in combination with

that of the plasma parameters, allowed the inference whether the satellite was inside or outside the foreshock region (Diodato et al., 1976).

(ii) When IMP 8 turned out to be inside the foreshock region, the occurrence of time fluctuations in the solar wind parameters was taken as an indication of the presence of the diffuse ions: this assumption is supported by the fact that solar wind parameters are known to fluctuate significantly in presence of the diffuse but not of the reflected ion population (Bonifazi et al., 1979; Formisano et al., 1979; Bame et al., 1979).

In Figure 4, the white and black bars indicate the presence of diffuse ions respectively at IMP 8 and ISEE 2 locations. When diffuse ions were absent, the two satellites turned out to be outside the foreshock region (reflected ions were never observed during the period considered). Note that the time interval shown partially overlaps with that already considered in the upper part of Figure 3. The sketch in the lower part of the Figure 4 (panel (b)) shows the position of the two satellites: it is seen that they were located outside the Earth's bow shock on opposite sides with respect to the Sun-Earth line (ISEE 2 in the dawn and IMP 8 in the dusk quadrant). The deceleration of the solar wind related to the diffuse ion population is fully confirmed (panel (a) of the figure): until 6:10 U.T. ISEE 2 (which was outside the foreshock region) measured a higher (and steadier) velocity than IMP 8 (which was inside the region filled by the diffuse ions); after that time, due to a change in the interplanetary magnetic field direction, the situation was reversed, with IMP 8 outside and ISEE 2 inside the foreshock region. (Note that in this figure, as well as thereafter in this section, the bulk velocities measured by IMP 8 were normalized to the ISEE 2 velocities using the equation:

$$V_{\text{IMP 8-normalized}} = (V_{\text{IMP 8}} - 14.8)/0.984 \text{ (km/s)} \qquad (1)$$

Therefore, velocity differences appearing in the plots cannot have an instrumental origin).

Figure 5 refers to the same period of time shown in the lower part of Figure 3. The increase of the solar wind velocity, apparently connected with the detection of the backstreaming ions, is now easily understood. At ∿ 10:30 U.T., a variation of the solar wind parameters (a velocity increase from ∿ 310 km/s to ∿330 km/s and a density decrease from ∿8 cm^{-3} to ∿5 cm^{-3}, according to IMP 8 observations) resulted in a ∿30% decrease of the dynamic pressure: as a consequence, the earth's bow shock moved outwards bringing ISEE 2 (but not IMP 8) within the foreshock region. At ∿ 16:00 U.T. the solar wind dynamic pressure again attained its previous high values and ISEE 2 returned into the unperturbed interplanetary space. When both spacecraft were outside the foreshock region, velocities are in close agreement; on the other hand, when ISEE 2 entered the region filled by the diffuse ions, $V_{\text{IMP 8}}$ is, on the average, ∿10 km/s larger than $V_{\text{ISEE 2}}$. This example, while confirming the proposed deceleration, evidences the ambiguities, which are unavoidably associated with the use of data taken from a single spacecraft.

To gain more information on the actual amount of the solar wind deceleration, we have investigated this phenomenon by performing an extended statistical analysis. We have selected several time intervals during which one satellite was in the presence of the diffuse ions while the other was observing the unperturbed solar wind outside the foreshock region. Data were then divided into two groups according to which satellite was in presence of the diffuse ion population. Group 1 (IMP 8 inside the foreshock region) consisted of 267 pairs of velocity measurements; group 2 (ISEE 2 inside the foreshock region) consisted of 283 pairs.

The results of the analysis are summarized in Figures 6, 7 and 8. Figure 6 displays scatter plots of velocities measured simultaneously by the two spacecraft: the two panels refer respectively to the two groups of data defined above. In panel (a), $V_{ISEE\ 2}$ is systematically higher than $V_{IMP\ 8}$ (the last velocity has been normalized, using equation (1)); the situation reverses in panel (b). On the average, it is found:

Group 1: $\langle V_{ISEE\ 2} \rangle$ = 332 km/s ; $\langle \Delta V \rangle$ = -9.9 km/s

Group 2: $\langle V_{IMP\ 8} \rangle$ = 363 km/s ; $\langle \Delta V \rangle$ = -11.3 km/s

(ΔV being the velocity decrease in the foreshock region).
Averaging over both groups of data, the deceleration turns out to be $\langle \Delta V \rangle$ = -10.7 km/s.

A more careful inspection of Figure 6 suggests that $|\Delta V|$ increases with the solar wind bulk velocity. This trend seems to be present in both groups of data. To show the effect more clearly, we have plotted ΔV as a function of V (Figure 7). The two sets of data have been superimposed to increase the statistical significance of the results. Bars are averages performed over 25 km/s velocity intervals. It is seen that ΔV increases from $\sim$-5 km/s (at V = 250÷300 km/s) up to $\sim$ -30 km/s (at V = 400÷450 km/s, the highest speeds used in our study). Correspondingly, the ratio $\Delta V/V$ changes from $\sim$0.01 up to $\sim$0.06: therefore, the data indicate that the increase of ΔV with V is even faster than linear. Figure 8 shows a histogram of the values of $\Delta V/V$. The average value of this ratio, indicated by the arrow in the figure, is: $\langle \Delta V/V \rangle \simeq$ 0.03.

4. SOLAR WIND FLOW DIRECTION

A search for a deflection of the solar wind flow associated with the presence of diffuse ions can also be performed by taking advantage of the dual satellite technique. The significance of such an analysis is ensured by the good agreement existing, on the average, between the flow directions measured by ISEE 2 and IMP 8, when both satellites are outside the foreshock region (Figure 1).

Data recorded by ISEE 2 and IMP 8 on day 335 (1977), during the same time interval already discussed in the previous section, offer a very favorable opportunity for testing the actual occurrence of a deflection of the solar wind flow in the foreshock region (panel (c) of Figure 4).

As already mentioned, before ∿ 6:10 U.T., the magnetic field direction was such that ISEE 2 was lying outside the foreshock region while IMP 8 was inside it; then the situation reversed (ISEE 2 inside the foreshock region and IMP 8 outside it). The strong fluctuations of the solar wind direction observed by IMP 8 until 6:10 U.T. and by ISEE 2 thereafter, clearly confirm that (when inside the foreshock region) the satellites were in presence of the diffuse ion population.

Concerning the average flow direction, the inspection of the figure shows:

(i) The directions of the solar wind measured by ISEE 2 until 6:10 U.T. are in very close agreement with those measured thereafter by IMP 8.

(ii) The average direction measured by IMP 8 until 6:10 U.T. is shifted towards negative values (i.e. towards the west) with respect to the unperturbed solar wind direction observed by ISEE 2.

(iii) The average direction measured by ISEE 2 after 6:10 U.T. is shifted towards positive values (i.e. towards the east) with respect to the unperturbed solar wind direction observed by IMP 8.

Point (i) confirms the consistency of the measurements performed by the two spacecraft. Points (ii) and (iii) indicate, on the other hand, that, when the diffuse ions are present, the solar wind flow is deflected away from the bow shock in agreement with what suggested by Bame et al., 1979 (see Section 1).

To evaluate quantitatively the amount of this deflection, we have performed a statistical analysis based on the same set of data already used in the previous section. The 550 pairs of direction measurements were divided into two groups according to the following criterion: Group 1 included cases when the satellite located inside the foreshock region was in the dusk quadrant; group 2 those when the satellite lying inside the foreshock region was in the dawn quadrant. (Note that, due to the geometry of its orbit, during the period of time considered here, ISEE 2 was never in the dusk quadrant, when inside the foreshock region).

Figure 9 summarizes the results of this analysis in the form of histograms. The trend suggested above is confirmed: in fact, the solar wind appears to be deflected towards the west on the dusk side of the shock (panel (a) of the figure) and towards the east on the dawn side (panel (b)). The average amounts of the deflection (arrows in the figure) are respectively: $\langle \Delta\phi \rangle = -1.3°$ (Group 1) and $\langle \Delta\phi \rangle = 0.9°$ (Group 2). We can conclude that the solar wind, when in presence of the diffuse ions, deviates from its unperturbed direction by $\sim 1°$ away from the direction of the earth's bow shock.

5. DISCUSSION

The analysis developed in Section 3 indicates that, when diffuse ions are present, the solar wind velocity decreases, on the average, by ~ 10 Km/s. An order of magnitude estimate of the kinetic energy loss (per proton) corresponding to this deceleration is:

$$\Delta E_k = 1/2\ m_p\ [(V + \Delta V)^2 - V^2] = -40\ eV \qquad (2)$$

(where we have assumed V = 380 km/s and ΔV = -10 km/s).

It is interesting to compare $|\Delta E_k|$ with the typical thermal energy (E_t) of the solar wind proton. Assuming W = 25 km/s, one gets:

$$E_t = 3/2\ m_p\ W^2 = 16\ eV \qquad (3)$$

i.e., ΔE_k is, in absolute value, about two and a half times E_t.

Therefore, if the entire kinetic energy loss in the deceleration process went into thermalization of the solar wind itself, we would expect a substantial increase in its temperature. In fact, such a temperature increase should be so large that it would stand out in a simultaneous comparison of the observations performed by IMP 8 and ISEE 2, despite the relatively poor correlation existing between their thermal speed measurements (Figure 2b).

We have investigated this problem through a statistical analysis based on the same set of 550 data pairs already considered in the previous sections. For each pair, we have computed the difference between kinetic (ΔE_k) and thermal (ΔE_t) energies (per proton) measured simultaneously outside and inside the foreshock region.

The results are summarized in the form of histograms in Figure 10. It is seen that a large difference exists, on the average, among the absolute values of ΔE_k and ΔE_t ($\langle \Delta E_k \rangle$ = -36 eV, $\langle \Delta E_t \rangle$=+3 eV). Thus the possibility that the kinetic energy lost is fully converted into thermal energy of the solar wind itself is ruled out.

It should be noted, however, that, due to the uncertainties inherent to the comparison of temperatures measured by the two spacecraft, we cannot exclude that a significant thermalization of the solar wind results from interaction with the diffuse ions. The slight asymmetry of the ΔE_t histogram ($\langle \Delta E_t \rangle$ = +3 eV) could indeed be taken as an indication that some thermalization actually occurs. What we would like to stress is that such a thermalization, if any, cannot account for the whole kinetic energy lost by the solar wind.

The kinetic energy, which apparently disappeared, could be of crucial importance in understanding other phenomena related to the interaction of the solar wind with the backstreaming ions. At present, the energy balance of the complex wave particle interactions occurring in the foreshock region is largely unknown. On the other hand, this problem is closely coupled to the origin of the diffuse ion population.

Some experimental evidence (Paschmann et al., 1979; Bonifazi et al., 1979) seems to be consistent with the following qualitative picture of the phenomena. Beams of "reflected" ions (characterized by sharply peaked energy spectra and by relatively collimated flow) are generated at the bow shock and interact with the solar wind producing, e.g., via the Barnes, 1970 mechanism, low frequency hydromagnetic waves. These waves may constitute the way for a momentum transfer from the beam to the solar wind determining the deceleration of both these flows (Bame et al., 1979). The observed deflection of the wind direction $\sim 1^\circ$ away from the bow shock would also be caused by such a transfer

of momentum (as reflected ions move along the interplanetary magnetic field lines). The diffuse ion population (characterized by flat energy spectra and broad angular distributions) should then be the result of the disruption of the reflected beams.

Even though attractive, this picture is far from being well established: a careful check of both the momentum and energy balance would be a very important test for the proposed theory. The results obtained above supply part of the basic information needed to undertake this test. The other pieces of information are expected to come from a detailed analysis of the backstreaming ions (both reflected and diffuse) and of the hydromagnetic waves.

A final comment concerns the apparent increase of the solar wind deceleration with the increasing bulk velocity. A qualitative explanation for this effect may be proposed in terms of the velocity of the solar wind relative to the backstreaming ions: higher solar wind velocities (and correspondingly higher velocities of the backstreaming ions) result in larger relative velocities which, in turn, may produce a stronger interaction between the two beams of particles.

6. CONCLUSIONS

The main conclusions reached in this paper may be summarized as follows:

(i) The two-spacecraft technique established unambiguously that, in the presence of "diffuse" ions, the solar wind decelerates, on the average, by $\Delta V \simeq 10$ km/s and is deflected by $\sim 1°$ away from the direction of the earth's bow shock.

(ii) The magnitude of the deceleration depends on the bulk velocity, with ΔV varying from $\sim$5 km/s ($V < 300$ km/s) up to $\sim$30 km/s ($V > 400$ km/s).

(iii) Even though some thermalization of the solar wind may occur in the presence of the diffuse ions, the kinetic energy ΔE_k, which is lost in the deceleration, far exceeds the thermal energy ΔE_t, which is possibly gained ($\langle|\Delta E_k|\rangle = 36$ eV/proton, $\langle|\Delta E_t|\rangle = 3$ eV/proton). Thus, at least part of the energy represented by the decrease in bulk velocity of the solar wind must go into waves and/or in the backstreaming ions.

ACKNOWLEDGEMENTS

It is a pleasure to acknowledge very useful discussions with H. Bridge, A. Egidi and J.T. Gosling. For use of UCLA magnetic field data from ISEE 1 we are indebted to C.T. Russell.

This research has been supported by the Consiglio Nazionale delle Ricerche of Italy and by the National Aeronautics and Space Administration under contract NAS5-11062 (GSFC).

REFERENCES

Auer, R.D., Grunwaldt, H., Rosenbauer, H.: "Bow shock associated proton heating in the upstream solar wind"
J. Geophys. Res. 81, 2030 (1976).

Bame, S.J., Asbridge, J.R., Felthauser, M.E., Glore, J.P., Paschmann, G., Hemmerich, P., Lehmann, K., Rosenbauer, H.: "ISEE 1 and 2 fast plasma experiment and the ISEE 1 solar wind experiment"
IEEE Trans. Geosci. Electron GE-16, 216 (1978).

Bame, S.J., Asbridge, J.R., Feldmann, W.C., Gosling, J.T., Paschmann, G., Sckopke, N.: "Deceleration of the solar wind upstream from the earth's bow shock and the origin of diffuse upstream ions"
Submitted to J. Geophys. Res. (1979).

Barnes, A.: "Theory of generation of bow-shock-associated hydromagnetic waves in the upstream interplanetary medium"
Cosmic Electrod. 1, 90 (1970).

Bavassano-Cattaneo, M.B., Bonifazi, C., Cerulli-Irelli, P., Diodato, L., Dobrowolny, M., Egidi, A., Orsini, S.: "Preliminary results from the solar wind experiment on the ISEE 2 satellite"
Space Science Reviews 23, 59 (1979).

Bellomo, A., Mavretic, A.: "MIT plasma experiment on IMP H and J earth orbited satellites"
Internal Report CSR TR-78-2, Center for Space Reaserch, Massachusetts Institute of Technology, Cambridge (Mass.) (1978).

Bonifazi, C., Cerulli-Irelli, P., Egidi, A., Formisano, V., Moreno, G.: "The EGD positive ion experiment on the ISEE-B satellite"
IEEE Trans. Geosci. Electron. GE-16, 243 (1978).

Bonifazi, C., Egidi, A., Moreno, G., Orsini, S.: "Backstreaming ions outside the earth's bow shock and their interaction with the solar wind"
J. Geophys. Res. in press (1979).

Diodato, L., Moreno, G.: "A two spacecraft study of the preshock perturbations of the solar wind protons"
J. Geophys. Res. 82, 3615 (1977).

Diodato, L., Greenstadt, E.W., Moreno, G., Formisano, V.: "A statistical study of the upstream wave boundary outside the earth's bow shock"
J. Geophys. Res. 81, 199 (1976).

Feldman, W.C., Asbridge, J.R., Bame, S.J.: "Bow shock perturbation of the upstream solar wind proton component"
J. Geophys. Res. 79, 2773 (1974).

Formisano, V., Amata, E.: "Solar wind interaction with the earth's magnetic field: 4. Preshock perturbation of the solar wind"
J. Geophys. Res. 81, 3907 (1976).

Formisano, V., Orsini, S., Bonifazi, C., Egidi, A., Moreno, G.: "High time resolution observations of the solar wind in the earth's foreshock region"
Geophys. Res. Letters, in press (1979).

Gosling, J.T., Asbridge, J.R., Bame, S.J., Paschmann, G., Sckopke, N.: "Observations of two distinct populations of bow shock ions in the upstream solar wind"
Geophys. Res. Lett. 5, 957 (1978).

Greenstadt, E.W.: "Binary index for assessing local bow shock obliquity"
J. Geophys. Res. 77, 5467 (1972).

Moreno, G., Signorini, C.: "Comparison of interplanetary plasma experiments"
ELDO/ESRO Scient. Tech. Rev. 5, 401 (1973).

Neugebauer, M.: "Initial deceleration of solar wind positive ions in the earth's bow shock"
J. Geophys. Res. 75, 717 (1970).

Paschmann, G., Sckopke, N., Bame, S.J., Asbridge, J.R., Gosling, J.T., Russell, C.T., Greenstadt, E.W.: "Association of low-frequency waves with suprathermal ions in the upstream solar wind" Geophys. Res. Lett. 6, 209 (1979).

FIGURE CAPTIONS

Figure 1.- Cross-comparisons of the values of proton bulk velocity (V) and azimuthal flow direction (Φ) measured simultaneously by ISEE 2 and IMP 8. Only periods when both satellites were in the undisturbed interplanetary space (i.e. outside the foreshock region) have been considered. The "ideal" correlation is represented by the broken straight lines, which pass through the origin and have a slope of 45°. Continuous straight lines, giving the best fit to the experimental points, have respectively equations:

$$V_{IMP\ 8} = 0.984\ V_{ISEE\ 2} + 14.8\ (km/s) \qquad (a)$$

$$\Phi_{IMP\ 8} = 1.017\ \Phi_{ISEE\ 2} - 0.12° \qquad (b)$$

Figure 2 - Same as figure 1 for the proton number density (N) and most probable thermal speed (W). Best fit straight lines have respectively equations:

$$N_{IMP\ 8} = 1.058\ N_{ISEE\ 2} + 2.24\ (cm^{-3}) \qquad (a)$$

$$W_{IMP\ 8} = 0.633\ W_{ISEE\ 2} + 10.4\ (km/s) \qquad (b)$$

Figure 3 - Time history of solar wind bulk velocity during the periods from U.T. 6:00 to U.T. 11:00 (Day 335, 1977) and from U.T. 9:00 to U.T. 18:00 (Day 342, 1977). For the first period of time measurements performed by both ISEE 1 (panel a) and ISEE 2 (panel b) are plotted, while for the second period only ISEE 2 measurements are given (panel c). ISEE 1 observations were performed by the LASL/MPI plasma experiment described by Bame et al., 1978. Black bars indicate periods of time when backstreaming ions of the diffuse population were detected.

Figure 4 - Simultaneous measurements of the solar wind bulk velocity (both magnitude and azimuthal direction) performed by ISEE 2 and IMP 8. The time interval considered, from U.T. 3:30 to U.T. 7:30 of Day 335, partially overlaps with that shown in panels (a) and (b) of Figure 3. White and black bars indicate the presence of diffuse ions respectively at IMP 8 and ISEE 2 locations. IMP 8 velocities were normalized to those measured by ISEE 2 through equation (1). Azimuthal directions (ϕ_{SW}) have not been corrected for the aberration due to the motion of the earth. Negative values of ϕ_{SW} denote flow from west of the Sun. The sketch in the lower part of the figure illustrates the positions of the two satellites (projected onto the X_{SE}-Y_{SE} plane) during the period considered.

Figure 5 - Simultaneous measurements of the solar wind bulk velocity performed by ISEE 2 and IMP 8 from 9:00 U.T. to 18:00 U.T. of Day 342. This time interval is coincident with that shown in panel (c) of Figure 3. As in the previous figure, white and black bars indicate the presence of diffuse ions respectively at IMP 8 and ISEE 2 locations; IMP 8 velocities were normalized to those measured by ISEE 2.

Figure 6 - Scatter plots of velocities measured simultaneously by ISEE 2 and IMP 8, when one satellite was inside and the other outside the foreshock region. Part (a) of the figure refers to cases when IMP 8 was inside and ISEE 2 outside the foreshock region (267 pairs of measurements); part (b) to the opposite situation (283 pairs). IMP 8 velocities were normalized to those measured by ISEE 2 using equation (1).

Figure 7 - The decrease of the solar wind bulk velocity (ΔV_{SW}), occurring in presence of the diffuse ion population, plotted against the bulk velocity itself. The two groups of data, considered separately in panels (a) and (b) of Figure 5, have been superimposed. Bars represent averages of ΔV_{SW} performed over 25 km/s velocity intervals.

Figure 8 - Histogram of the ratios $\Delta V_{SW}/V_{SW}$ for the same set of data considered in Figure 6. The average value of the ratio ($\langle \Delta V_{SW}/V_{SW} \rangle = 0.03$) is indicated by the arrow.

Figure 9 - Histograms of the azimuthal deflection of the solar wind flow ($\Delta\Phi_{SW}$), occurring in presence of the diffuse ion population. In panel (a) cases are considered when the satellite located inside the foreshock region was in the dusk quadrant (214 pairs of measurements); in panel (b) cases when the satellite inside the foreshock region was in the dawn quadrant (336 pairs). Positive values of $\Delta\Phi_{SW}$ correspond to a deflection of the solar wind flow towards the east of the Sun; negative values to a deflection towards the west. Average values of the deflections, indicated by the arrows, are respectively: $\langle \Delta\Phi_{SW} \rangle = -1.3°$ (panel a) and $\langle \Delta\Phi_{SW} \rangle = +0.9°$ (panel b).

Figure 10 - Histograms of the kinetic (ΔE_k) and thermal (ΔE_t) energies gained (or lost) by each solar wind proton in presence of the diffuse ions. Positive (negative) values of ΔE correspond to gain (lost) of energy. The average values of ΔE_k and ΔE_t, indicated by the arrows, are respectively: $\langle \Delta E_k \rangle = -36$ eV, $\langle \Delta E_t \rangle = +3$ eV.

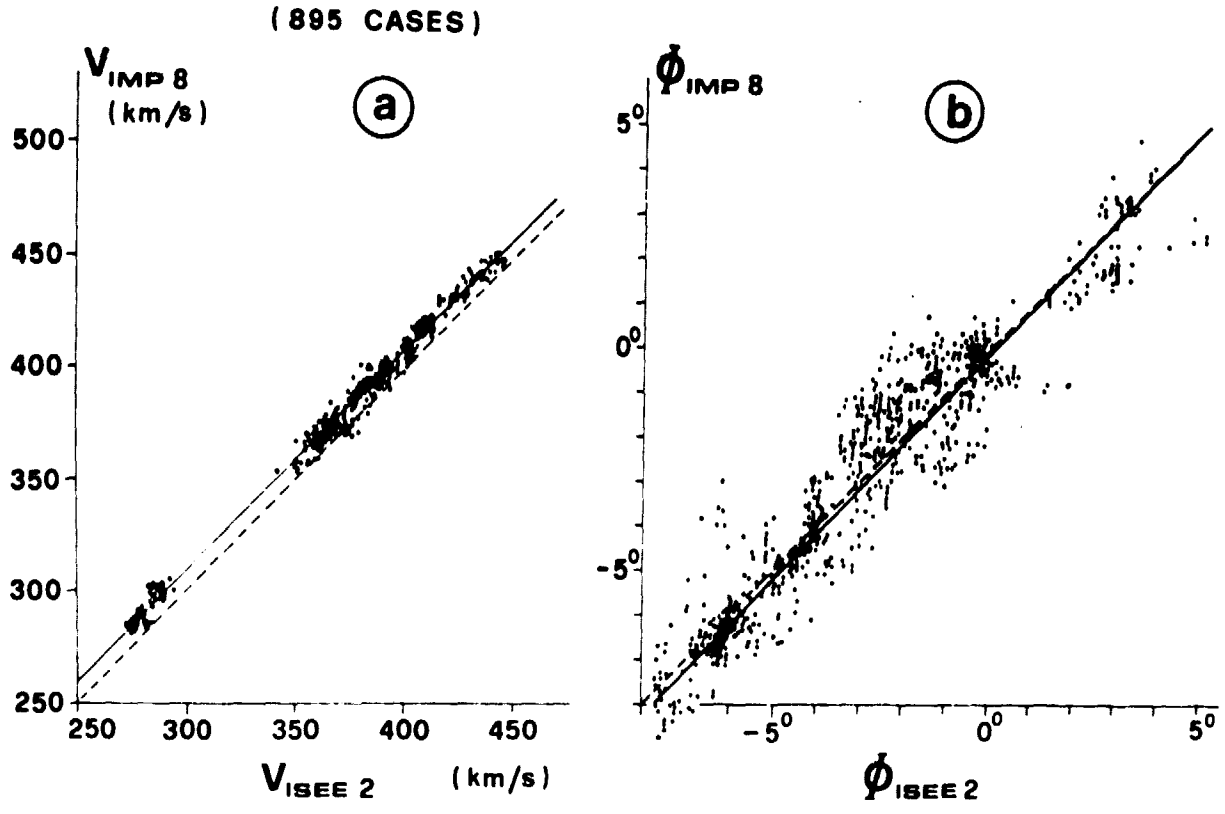
(895 CASES)
$V_{IMP\ 8}$ (km/s)
a
500
450
400
350
300
250
250 300 350 400 450
$V_{ISEE\ 2}$ (km/s)
$\phi_{IMP\ 8}$
b
5^0
0^0
-5^0
-5^0 0^0 5^0
$\phi_{ISEE\ 2}$

FIG. 1

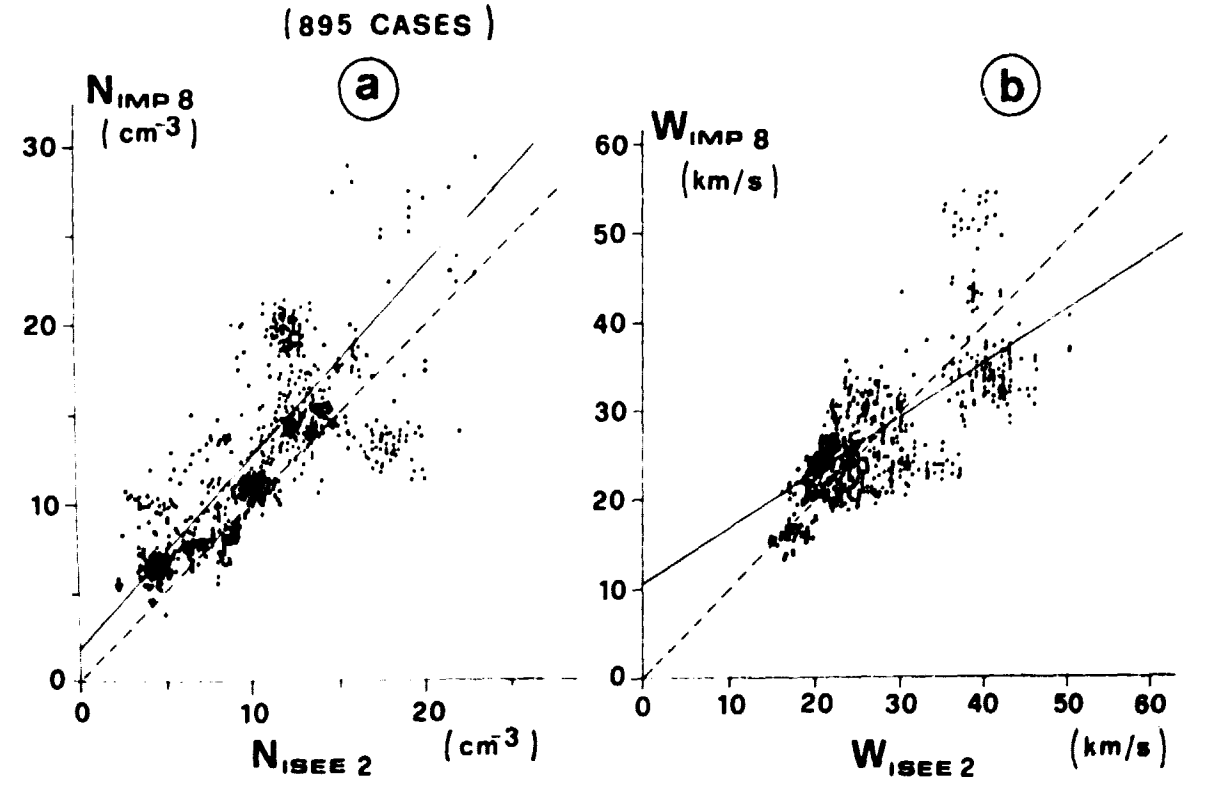
(895 CASES)
$N_{IMP\ 8}$ (cm^{-3})
a
30
20
10
0
0 10 20
$N_{ISEE\ 2}$ (cm^{-3})
$W_{IMP\ 8}$ (km/s)
b
60
50
40
30
20
10
0
0 10 20 30 40 50 60
$W_{ISEE\ 2}$ (km/s)

FIG. 2

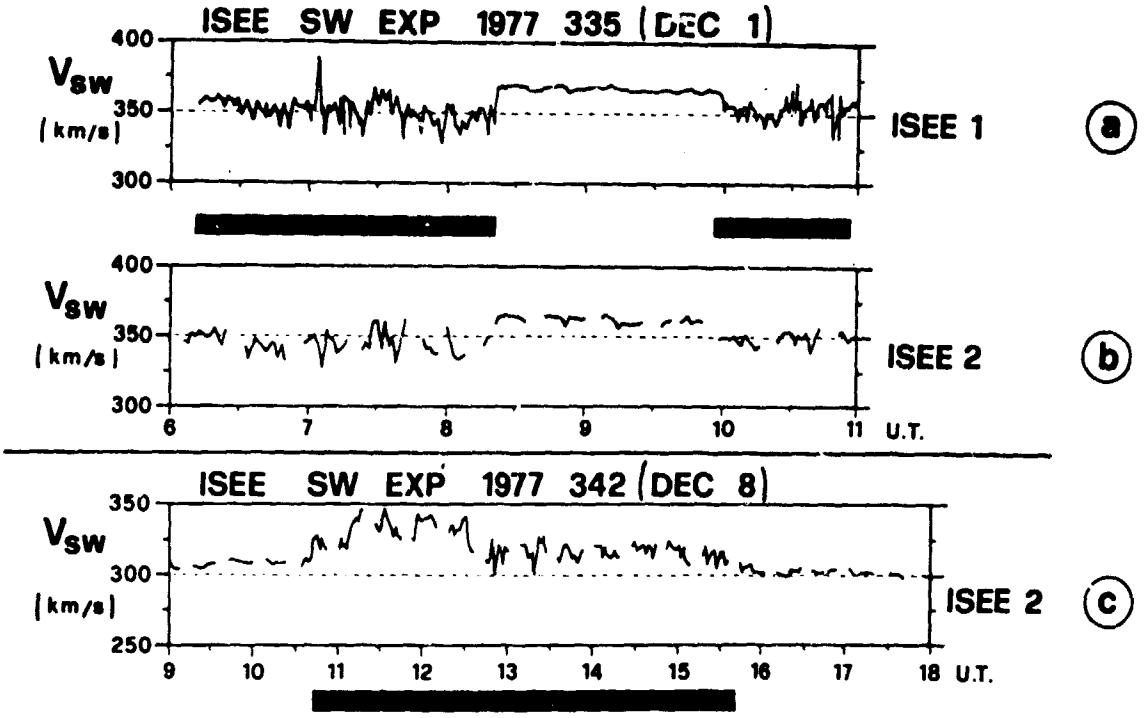
ISEE SW EXP 1977 335 (DEC 1)
V_{SW}
(km/s)
400
350
300
ISEE 1
a
ISEE 2
b
6
7
8
9
10
11
U.T.
ISEE SW EXP 1977 342 (DEC 8)
350
300
250
ISEE 2
c
9
10
11
12
13
14
15
16
17
18
U.T.

FIG. 3

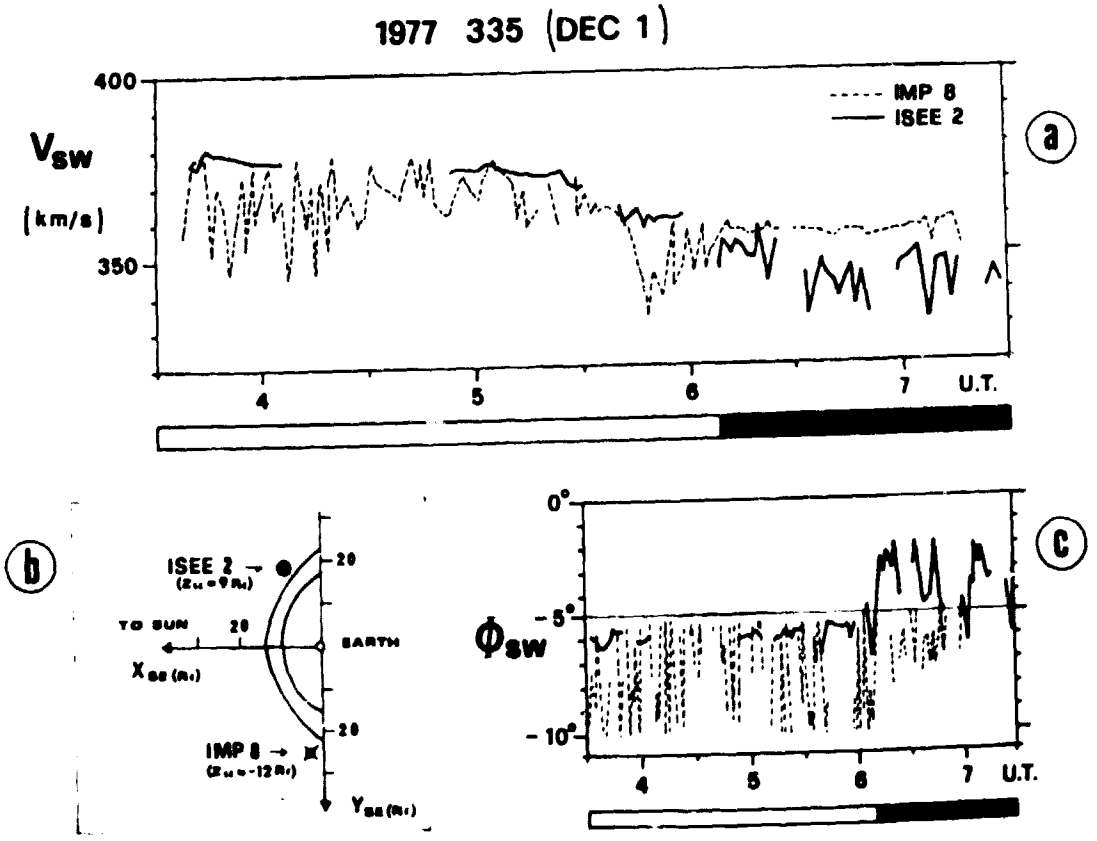
1977 335 (DEC 1)
400
350
V_{SW}
(km/s)
IMP 8
ISEE 2
a
4
5
6
7
U.T.
b
ISEE 2
TO SUN
20
EARTH
X_{SE}
IMP 8
Y_{SE}
0°
-5°
-10°
Φ_{SW}
c

FIG. 4

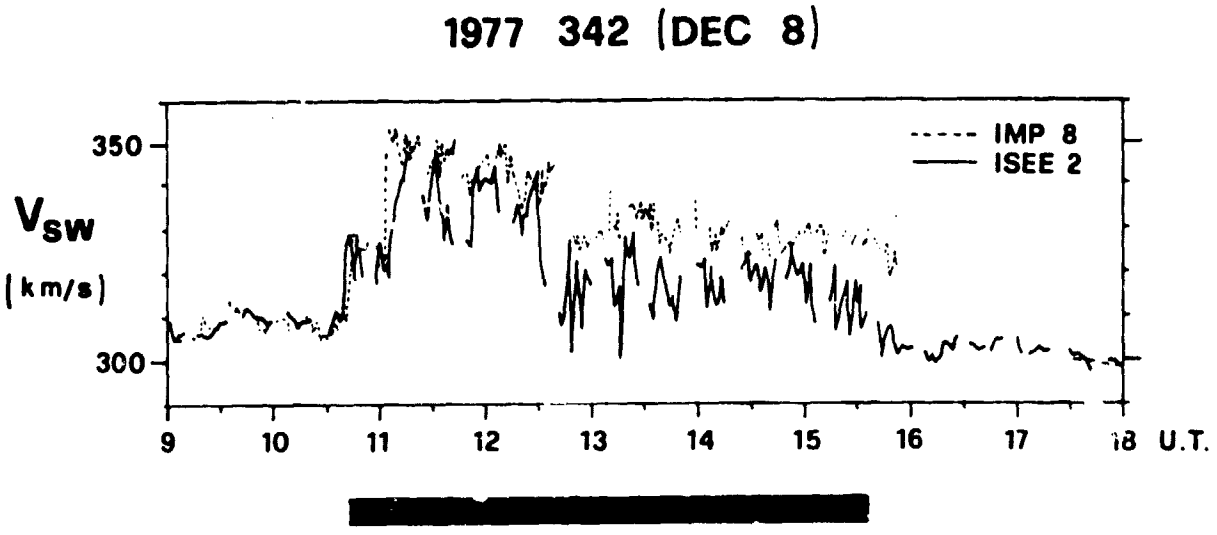
1977 342 (DEC 8)
IMP 8
ISEE 2
V_{SW}
(km/s)
350
300
9
10
11
12
13
14
15
16
17
18 U.T.

FIG. 5

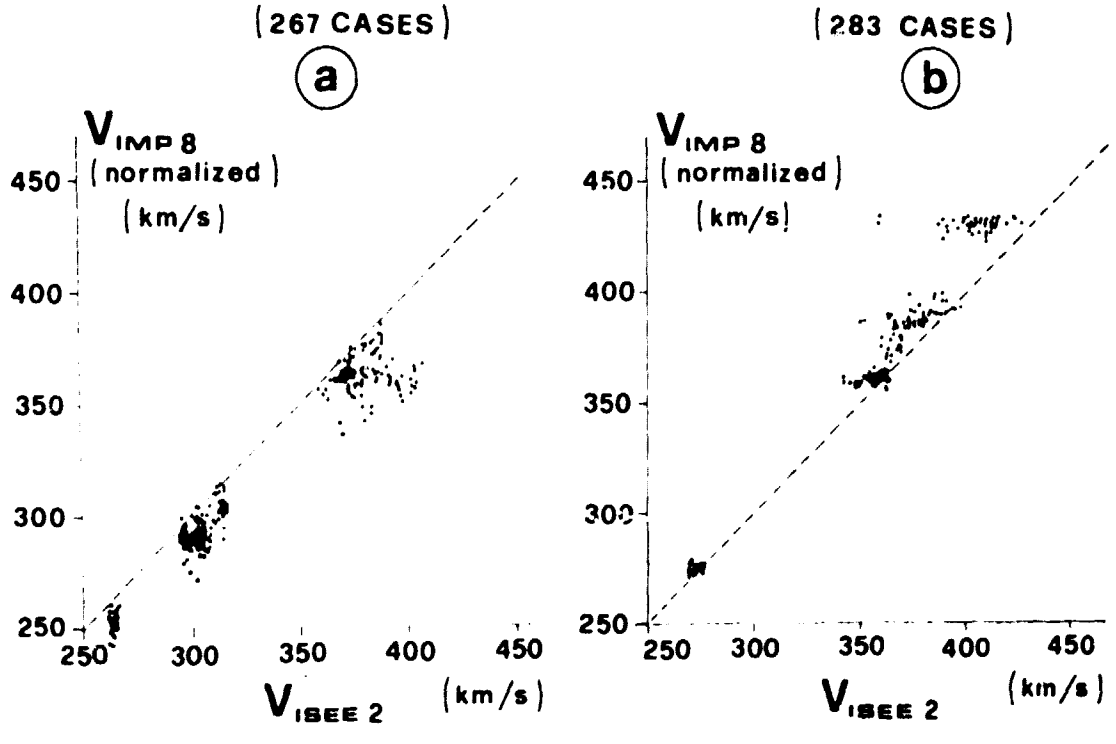
(267 CASES)
a
$V_{IMP\ 8}$
(normalized)
(km/s)
450
400
350
300
250
250
300
350
400
450
$V_{ISEE\ 2}$
(km/s)
(283 CASES)
b
$V_{IMP\ 8}$
(normalized)
(km/s)
450
400
350
300
250
250
300
350
400
450
$V_{ISEE\ 2}$
(km/s)

FIG. 6

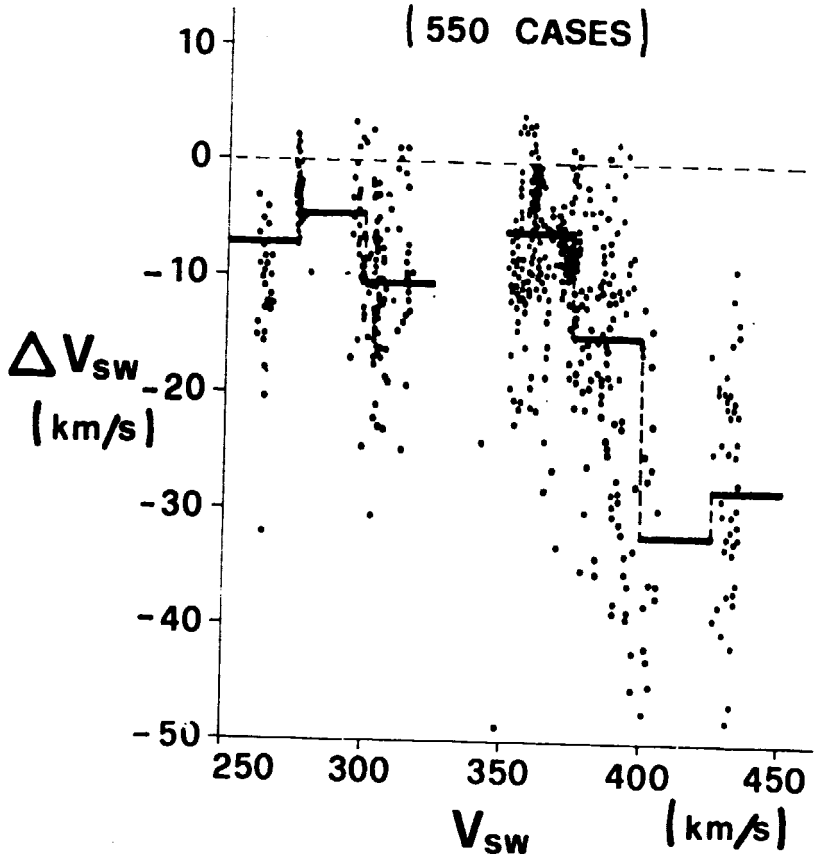
(550 CASES)
10
0
-10
-20
-30
-40
-50
ΔVsw
(km/s)
250
300
350
400
450
Vsw
(km/s)

FIG. 7

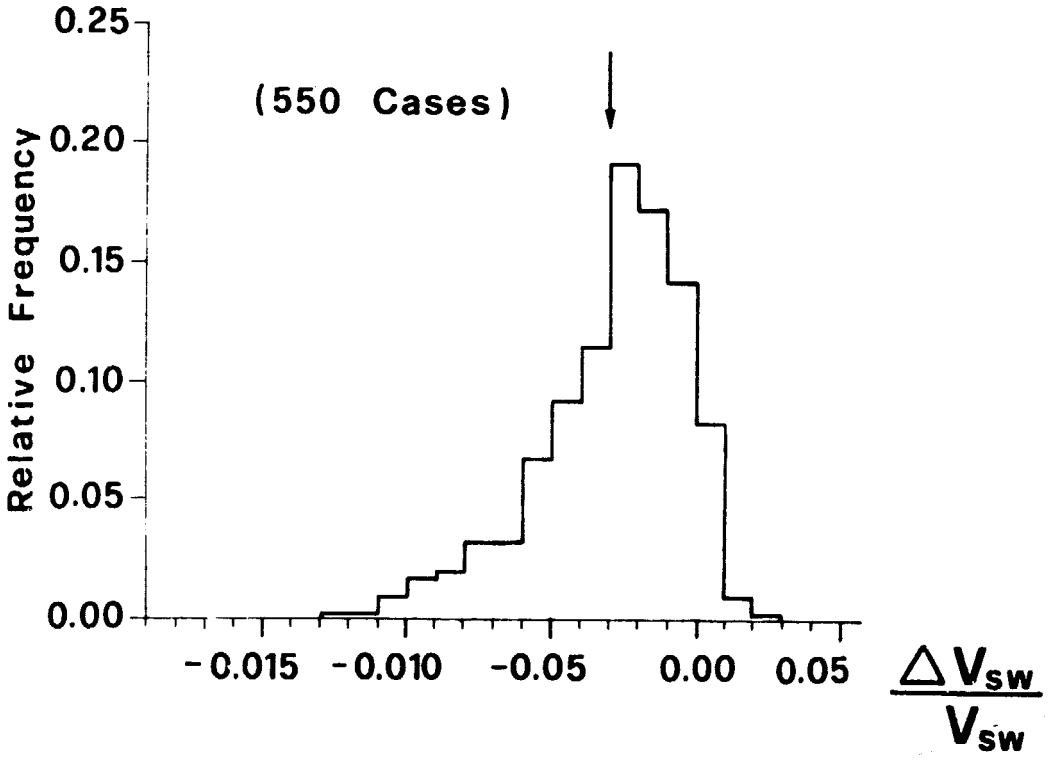
0.25
0.20
0.15
0.10
0.05
0.00
Relative Frequency
(550 Cases)
-0.015
-0.010
-0.05
0.00
0.05
ΔVsw
Vsw

FIG. 8

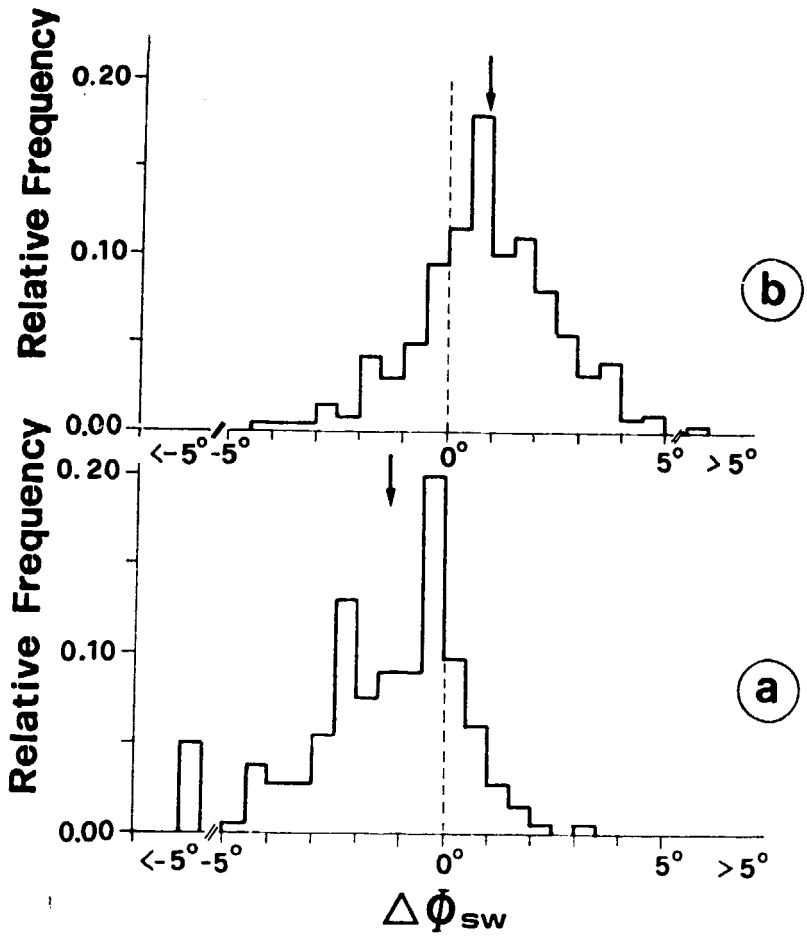
Relative Frequency
0.20
0.10
0.00
b
<-5°
-5°
0°
5°
>5°
Relative Frequency
0.20
0.10
0.00
a
<-5°
-5°
0°
5°
>5°
Δφsw

FIG. 9

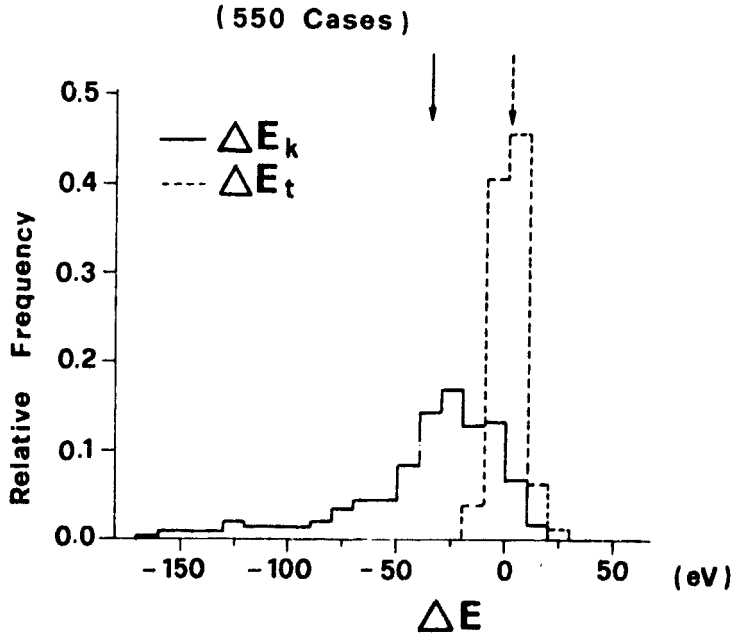
(550 Cases)
ΔEk
ΔEt
Relative Frequency
0.5
0.4
0.3
0.2
0.1
0.0
-150
-100
-50
0
50
(eV)
ΔE

FIG. 10